Layer Ordering and Faulting in $(GaAs)_n/(AlAs)_n$ Ultrashort-Period Superlattices

J. H. Li,[1,2] S. C. Moss,[1,2] Y. Zhang,[3] A. Mascarenhas,[3] L. N. Pfeiffer,[4] K. W. West,[4] W. K. Ge,[5] and J. Bai[6]

[1]*Physics Department, University of Houston, Houston, Texas 77204-5005, USA*

[2]*Texas Center for Superconductivity and Advanced Materials, University of Houston, Houston, Texas 77204, USA*

[3]*National Renewable Energy Laboratory, Golden, Colorado 80401, USA*

[4]*Bell Laboratories, Lucent Technology, Murray Hill, New Jersey 07974, USA*

[5]*Department of Physics, Hong Kong University of Science & Technology, Hong Kong, China*

[6]*Oak Ridge National Laboratory, Oak Ridge, Tennessee 37831, USA*

(Received 24 February 2003; published 5 September 2003)

We report studies of $(GaAs)_n/(AlAs)_n$ ultrashort-period superlattices using synchrotron x-ray scattering. In particular, we demonstrate that interfaces of these superlattices contain features on two different length scales: namely, random atomic mixture and ordered mesoscopic domains. Both features are asymmetric on the two interfaces (AlAs-on-GaAs and GaAs-on-AlAs) for $n > 2$. Periodic compositional stacking faults, arising from the intrinsic nature of molecular-beam epitaxy, are found in the superlattices. In addition, the effect of growth interruption on the interfacial structure is discussed. The relevant scattering theory is developed to give excellent fits to the data.

DOI: 10.1103/PhysRevLett.91.106103 PACS numbers: 68.65.Cd, 61.10.Eq, 61.10.Nz, 68.55.–a

The development of molecular-beam epitaxy (MBE) has permitted the growth of semiconductor heterostructures with monatomic-layer accuracy. The ultimate test for such an outcome may be the growth of ultrashort-period superlattices (USPS) with one or a few monolayers (ML) for each constituent. To this end, $(GaAs)_n/(AlAs)_n$ with $n = 1$–4 has been commonly used as a prototype system [1]. On the other hand, it has been demonstrated that epitaxial growth of semiconductor III-V ternary alloys can lead to spontaneously ordered USPS's [2,3]. For instance, partially ordered $(Ga_{0.5+S/2}In_{0.5-S/2}P)_1/(Ga_{0.5-S/2}In_{00.5+S/2}P)_1$ USPS's can form in a $Ga_{0.5}In_{0.5}P$ alloy with a maximum order parameter $S < 0.6$. Even though some interlayer diffusion may occur, one would still expect a higher degree of ordering in the artificial $(GaAs)_n/(AlAs)_n$ USPS system. Apart from extensive experimental and theoretical studies on MBE grown $(GaAs)_n/(AlAs)_n$ USPS's over the past decade [1], a marked disagreement between experiment and theory has remained unsettled to date, although some hypotheses have been proposed [4]. Therefore, a clear understanding of the GaAs-AlAs USPS structure on an atomistic level is of great interest for (1) obtaining a comprehensive insight into the ordering phenomenon in semiconductor alloys; (2) providing fundamental knowledge essential for understanding the disagreement between experiment and theory; and, more importantly, (3) exploring sources of imperfections in the USPS's and suggesting possible ways for improvement.

Early photoluminescence (PL) experiments on $GaAs/Al_xGa_{1-x}As$ quantum wells (QW) have indicated the existence of discrete thickness fluctuations of the QW on a lateral scale larger than the exciton diameter [5]. Subsequent high-resolution transmission electron microscopy (HRTEM) experiments, however, failed to observe these large, atomically flat islands [6]. On the other hand, Raman scattering studies of GaAs/AlAs USPS's have revealed an asymmetric structure of the normal (AlAs-on-GaAs) and the inverted (GaAs-on-AlAs) interfaces in terms of compositional roughness, which strongly suggests cation intermixing at the interface due to Ga segregation [7]. This asymmetric atomic segregation at the two interfaces was confirmed by *in situ* reflection high-energy electron diffraction (RHEED) experiments [8]. Recent cross-sectional scanning tunneling microscopy (XSTM) experiments showed, in a 20–40 nm length scale, small islands of several unit cells at both interfaces [9]. Apart from these somehow contradictory experimental results, a bimodal roughness spectrum, based on cathodoluminescence (CL) measurements, has also been proposed for $GaAs/Al_xGa_{1-x}As$ QW interfaces [10], which assumes that the interface consists of both large atomically flat islands (> 60 nm) and atomic-scale compositional roughness within the islands. The HRTEM experiments, however, suggest that these large CL features should arise from clusters of many small islands [6].

In this Letter, we report an x-ray scattering study of $(GaAs)_n/(AlAs)_n$ ($n = 1$, 2, and 4) USPS's, hereafter referred to as n/n superlattices. We show unambiguously that these USPS's consist of features on two different length scales: namely, random atomic mixture and ordered mesoscopic domains. Moreover, no interface asymmetry was observed in samples with $n \leq 2$. For $n = 4$, the normal and inverted interfaces are asymmetric on both length scales. In addition, we show that growth interruption improves the interface quality by facilitating growth of larger mesoscopic islands. Our results also reveal that there is a periodic compositional stacking-fault (CSF) structure in the USPS's arising from an intrinsic property of the MBE growth.

$(GaAs)_n/(AlAs)_n$ USPS's were grown by MBE on undoped GaAs (001) substrates at a temperature of 500 °C

and a deposition rate of 1 Å/s [7]. The substrates are virtually nonvicinal (the miscut is $<0.15°$). A 300 nm GaAs buffer was grown at 650 °C prior to the USPS growth. The USPS periods of the $n = 1$, 2, and 4 samples are 1000, 500, and 200, respectively. All superlattices were grown continuously except with one of the two samples with $n = 1$, which was grown with an interruption of 10 s after deposition of each. The x-ray measurements were performed at the National Synchrotron Light Source with an x-ray energy of 8.0478 keV. The x-ray sampling size is about 0.2×0.2 mm^2.

The experimental x-ray results are quite surprising. For a 1/1 superlattice, the superstructure peaks, or satellites, along the (00l) rod should appear at positions where l is an odd integer, such as 1 or 3, in which case: (1) The superlattice is perfect, the x-ray satellite peaks are strong and sharp, and their intensities are solely determined by the contrast between the atomic form factors of Ga and Al. (2) The Ga and Al ions are uniformly intermixed. The satellite peaks will remain sharp, but their intensities are reduced by a factor of S^2 ($0 \leq S \geq 1$). Thus, the nominal GaAs (AlAs) layer is actually a $Ga_{0.5+S/2}Al_{0.5-S/2}As$ ($Al_{0.5+S/2}Ga_{0.5-S/2}As$) alloy. In the case of $S = 0$, the two layers are completely intermixed and the superlattice becomes a uniform alloy $Ga_{0.5}Al_{0.5}As$, for which there will be no satellite reflections. However, our experimental results, shown in Fig. 1, differ markedly from these limiting situations. The expected (003) superlattice peak splits into two peaks at (0, 0, 2.967) and (0, 0, 3.033), and these split peaks are considerably broadened along the in-plane [110] direction.

For a perfect 2/2 superlattice, satellites would be located only at $(0, 0, \frac{l}{2})$, where l is an odd integer. If the two cations intermixed uniformly at the interfaces, there would be the following two possibilities: (1) The two GaAs (AlAs) layers are equivalent. Then, weakened $(0, 0, \frac{l}{2})$ peaks are expected but no (00l) peaks should appear. (2) The two GaAs (AlAs) layers differ from each other due to their different neighboring environments in which case the (00l) peaks should appear in addition to the $(0, 0, \frac{l}{2})$ peaks. We have measured the x-ray reflections around the $(0, 0, \frac{5}{2})$, (003), and $(0, 0, \frac{7}{2})$ reciprocal lattice points. Indeed, no (003) reflection is detected, indicating that there is no measurable difference between the two GaAs (or AlAs) layers within our experimental resolution. On the other hand, the $(0, 0, \frac{5}{2})$ and $(0, 0, \frac{7}{2})$ peaks are found slightly, but clearly, displaced to (0, 0, 2.487) (Fig. 2) and (0, 0, 3.513) (not shown), respectively; these 2/2 peaks, however, now remain unsplit. Nonetheless, similar to the 1/1 superlattice, the displaced reflections are broadened along the [110] direction.

The rod scan of the 4/4 superlattice is shown in Fig. 3. In addition to the first- and the second-order satellites, unexpected extra peaks are observed between the satellites. We note that if the 4 MLs of GaAs (or AlAs) were equivalent, there would be no observable even order satellites. The observed second-order satellites are then a clear indication of nonequivalence of the 4 MLs GaAs

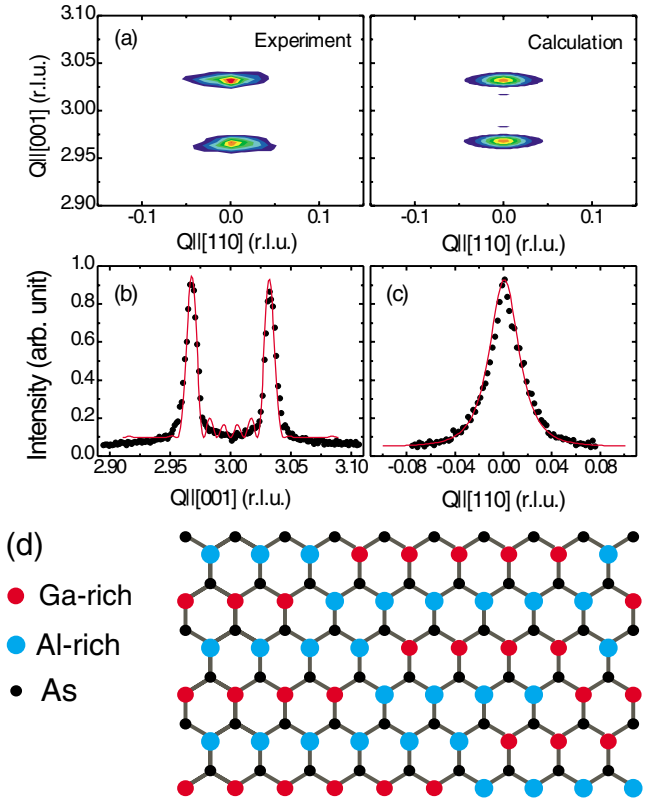

FIG. 1 (color online). (a) X-ray 2D scans around (003) of the 1/1 superlattice. The left-hand side (lhs) shows experimental data, and the right-hand side (rhs) shows calculations; (b) longitudinal and (c) transverse scans. Dots and lines are experimental and calculated data, respectively; (d) an atomic structural model of the 1/1 superlattice. The lateral domains are shown in a reduced length scale. The high frequency oscillation in (b) is due to finite film thickness interference.

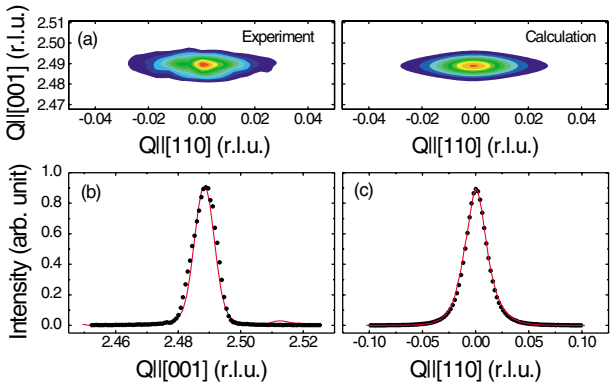

FIG. 2 (color online). (a) X-ray 2D scans around (0, 0, 2.5) of the 2/2 superlattice. The lhs shows experimental data, and the rhs shows calculations; (b) longitudinal and (c) transverse linear scans. Dots and lines are experimental and calculated data, respectively.

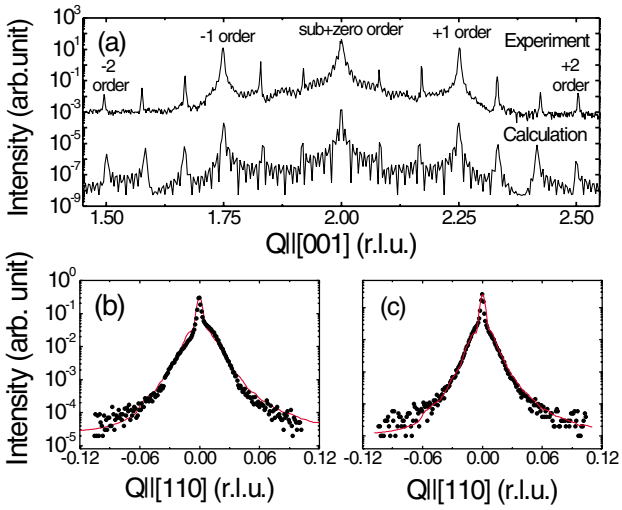

FIG. 3 (color online). (a) X-ray longitudinal scans around (002) of the 4/4 superlattice; (b),(c) transverse scans across the -1 and the $+1$ order satellites. Dots and lines are experimental and calculated data, respectively.

(AlAs). More interestingly, the transverse scans along [110] across the two first-order peaks consist of two components, a sharp one superimposed on a broad one.

It is well known that Ga segregates in the GaAs/AlAs systems [7,8]. This means that in our USPS's, the nominal GaAs (AlAs) layer may actually be a GaAs-rich (AlAs-rich) alloy. The splitting of the (003) peak in Figs. 1(a) and 1(b) then suggests that there are ''antiphase boundaries'' in the growth direction. The extra peaks in Fig. 3(a) also suggest that there is an additional long-period modulation. It has been shown that precise control of the MBE growth rate of a heterostructure is almost impossible as revealed, for example, in a phase shift of the RHEED oscillations at the heterointerfaces [8]. There is always an intrinsic small growth mistake which leads to a slight increase or decrease of deposited materials. Accumulation of these mistakes can result in periodic CSF's in the multilayer stack: namely, a certain designed GaAs (or GaAs-rich) layer can be actually AlAs rich and vice versa. Finally, the broadening of superlattice satellites along the [110] direction indicates a reduced lateral correlation length. In our superlattices, the only possible defect source arises from the two different group-III ions. We thus assume that each ML consists of GaAs-rich and AlAs-rich domains. Such a domain structure is quite realistic because of the nature of MBE growth. For example, steps in the growing film and/or nonplanar growth of AlAs are the two most probable origins. Therefore, the structure of a 1/1 superlattice should appear like the one shown in Fig. 1(d). A similar structure exists in the 2/2 and 4/4 superlattices. Since the 2 MLs of the same type in the 2/2 superlattice are equivalent and the 4 MLs of the same type in the 4/4 superlattice are not equivalent, the domain boundaries have to be about 1–2 MLs in extent. This dimension is in good agreement with that deduced from the PL measurements, which suggests 1–2 MLs discrete thickness fluctuations in the GaAs/Al(Ga)As superlattices or QWs [5].

We denote the three crystal axes as $\mathbf{a} \parallel [100]$, $\mathbf{b} \parallel [010]$, and $\mathbf{c} \parallel [001]$, where the superlattice was deposited along the $\mathbf{c}$ axis. The domain boundaries in Fig. 1(d) can then be attributed to half-diagonal glides involving displacements $(\mathbf{b} + \mathbf{c})/2$ and $(\mathbf{a} + \mathbf{c})/2$. If γ represents the possibility of crossing a domain boundary in a distance a, where a is the unit cell dimension of cubic GaAs, a/γ is the average size of the in-plane domains. For 2/2 and 4/4 structures, a full diagonal glide is also possible.

Now, consider a 2D structure factor F_{2D} of a single ML

$$F_{2D} = FG, \tag{1}$$

where F is the usual structure factor and G is a factor accounting the lateral domain boundaries. G of the reflection (hkl) may be written in the form [11]

$$G = \sum_{n_1} \sum_{n_2} \langle e^{i\phi(1)} \rangle^{|n_1|} \langle e^{i\phi(2)} \rangle^{|n_2|} e^{2\pi i n_1 h} e^{2\pi i n_2 k}, \tag{2}$$

where $\langle e^{i\phi(1)} \rangle$ and $\langle e^{i\phi(2)} \rangle$ denote average phase shifts across a unit cell boundary in the [100] and [010] directions, which for simplicity can be assumed to be the same. n_i $(i = 1, 2)$ is the distance between any two cells in the [100] and [010] directions, respectively.

The x-ray intensity can then be written as

$$I \propto \sum_{m} \sum_{m'} F_{2D,m} F^{*}_{2D,m'} e^{2\pi i (m-m')l}, \tag{3}$$

where m represents the mth ML. If the stacking of type A and B atomic layers of our superlattices follows a ''correct'' order $\{ABABAB\ldots\}$ or $\{AABBAABB\ldots\}$ or $\{AAAABBBB\ldots\}$, Eq. (3) can easily be evaluated. However, if there are periodic CSF's, whose wavelength is much larger than the superlattice period, the stacking sequence may become $\{ABAB\ldots AB|BABA\ldots BA|ABAB\ldots AB\ldots\}$ for the 1/1 superlattice, $\{AABB\ldots AABB|BAAB\ldots BA|AABB\ldots AABB\ldots\}$ for the 2/2 superlattice, and $\{AAAABBBB\ldots AAAABBBB|BAAABBBB\ldots AAAABBBA|AAAABBBB\ldots\}$ for the 4/4 superlattice. In this case, the superlattice can be regarded as consisting of two building blocks. Equation (3) can then be evaluated by considering these two-component blocks as constituents of a long-wavelength superstructure superimposed on the ordinary superlattice.

For the 1/1 superlattice, we consider a 1-ML perturbation at the interfaces as in Fig. 1(d). In the case of $h = k$ as in our experiments, the average phase factor is $\langle e^{i\phi(1)} \rangle = \langle e^{i\phi(2)} \rangle = \eta = 1 - \gamma + \gamma e^{i\pi(h+l)}$. For the 2/2 and 4/4 superlattices, a 2-ML perturbation also needs to be considered. Assuming the same probability, we then have $\langle e^{i\phi(1)} \rangle = \langle e^{i\phi(2)} \rangle = \eta = 1 - \gamma + \gamma[e^{i\pi(h+l)} + e^{i\pi(h-l)} + e^{i2\pi(h+l)} + e^{i2\pi(h-l)}]/4$. The G factor is now written as

$$G = 1 + \frac{\eta e^{2\pi i h}}{1 - \eta e^{2\pi i h}} + \frac{\eta e^{-2\pi i h}}{1 - \eta e^{-2\pi i h}}. \quad (4)$$

Equations (1)–(4) are used to simulate the x-ray spectra. The best fits to the experimental data are shown in Figs. 1–3, together with their experimental counterparts. The excellent agreement between the experimental and calculated data in Fig. 1 requires in the 1/1 superlattice that there is a CSF every 15 MLs, which accounts for the peak splitting and the absence of a peak at l = odd. The broadening of the split peaks along the [110] direction is now attributed to the 2D lateral domains of an average size of 11 unit cells. Comparing the intensities of the split peaks and the (002) reflection results in an order parameter, S, of about 0.1, which means that the alloy compositions of the two domains are about $Ga_{0.55}Al_{0.45}As$ and $Ga_{0.45}Al_{0.55}As$, respectively—a significant compositional intermixing inside the domains.

The fit to the x-ray data of the 2/2 superlattice (Fig. 2) shows that the origin of the peak shift is also due to the periodic CSF's, with a periodicity of about 12 MLs. The average lateral domain size is about 20 unit cells. As noted above, there is no distinguishable difference between the two "GaAs" (or "AlAs") layers. The average composition of the GaAs (AlAs) domain is determined to be $Ga_{0.58}Al_{0.42}As$ ($Ga_{0.42}Al_{0.58}As$). In the 1/1 superlattice, the CSF's reverse the phase from *AB* to *BA* and thus cause the splitting of the satellite peak. In the 2/2 superlattice, however, the CSF's result only in a shift of the structural phase, and consequently a shift of the satellite peak; no splitting is either observed or predicted.

The extra peaks in the (00l) rod scan of the 4/4 superlattice is again due to the CSF's of every 12 MLs, which imposes an additional long-wavelength modulation on the basic 4/4 structure. The observed two-component transverse scans [Figs. 3(b) and 3(c)] indicate that there are two distinct interfaces, one with a small domain size (broad component) and the other one with a large domain size (narrow component). The best fits to the experimental curves were obtained by assuming an average domain size of about 200 and 25 unit cells at the normal and inverted interfaces, respectively. The average Ga fraction of each ML of AlAs-type and GaAs-type is, from top to bottom, 0.2, 0.3, 0.4, 0.45, and 0.55, 0.6, 0.7, 0.8 ($\pm$ 0.04). We see that the composition is asymmetric at the normal and the inverted interfaces, whose profiles favor the Ga-segregation model proposed earlier [7,8].

Thus far, we have observed a two-length-scale feature of the interfaces in the GaAs/AlAs USPS's. The interfacial asymmetry appears when $n > 2$. We now explore the effect of growth interruption on the interfaces. A second 1/1 superlattice was grown with a 10 s break after deposition of each ML. The measured (003) peak also splits into two in a way similar to Fig. 1(a), but the peak width along the [110] direction is much narrower. Our analyses reveal that the order parameter, S, of this sample is about the same as that of the 1/1 superlattice without growth interruption. However, the size of the lateral domains in this sample is as large as 34 unit cells, which suggests that the growth interruption results in larger domains due to a sufficient migration of adatoms.

The existence of the CSF's in our samples suggests a growth rate error of about 5%–9% with respect to that monitored by RHEED. In fact, one XSTM experiment seems to have observed the absence of an atomic ML in the AlAs/GaAs USPS's [9], which may now be explained by our CSF model as a consequence of the growth rate error. Such an error may just contribute to the interface roughness of large period superlattices, indicating that growth of atomically flat heterointerfaces via current technology is intrinsically difficult. It should also be noted that, while in this work on USPS structures the antiphasing or faulting is better correlated in the growth direction than laterally, in our earlier study of spontaneously ordered $GaAs_xSb_{1-x}$ films exactly the opposite result obtained: namely, sharp peaks in [110] and extended streaking in [001] [12].

The work at UH is supported by NREL under Contract No. XDJ-2-32615-01, NSF with Grant No. DMR-0099573. NREL is a national laboratory operated by Midwest Research Institute, Battelle and Bechtel, for the U.S. Department of Energy under Contract No. DE-AC36-99GO10337.

[1] For a review, see W.-K. Ge *et al.*, J. Lumin. **59**, 163 (1994).
[2] P. Venezuela *et al.*, Nature (London) **397**, 678 (1999).
[3] *Spontaneous Ordering in Semiconductor Alloys*, edited by A. Mascarenhas (Kluwer Academics, New York, 2002).
[4] D. B. Laks and A. Zunger, Phys. Rev. B **45**, 11 411 (1992).
[5] B. Deveaud *et al.*, Appl. Phys. Lett. **45**, 1078 (1984); R. F. Kopf *et al.*, Appl. Phys. Lett. **58**, 631 (1991).
[6] A. Ourmazd *et al.*, Phys. Rev. Lett. **62**, 933 (1989); Ultramicroscopy **34**, 237 (1990).
[7] G. S. Spencer *et al.*, Phys. Rev. B **52**, 8205 (1995), and references therein.
[8] W. Braun and K. H. Ploog, J. Appl. Phys. **75**, 1993 (1993); W. Braun *et al.*, Phys. Rev. B **55**, 1689 (1997).
[9] A. R. Smith *et al.*, Appl. Phys. Lett. **66**, 478 (1994); J. Vac. Sci. Technol. B **13**, 1824 (1995).
[10] D. Bimberg *et al.*, J. Vac. Sci. Technol. B **5**, 1191 (1987); C. A. Warwick and R. F. Kopf, Appl. Phys. Lett. **60**, 386 (1992).
[11] B. E. Warren, *X-ray Diffraction* (Dover Publications, New York, 1990).
[12] Z. Zhong *et al.*, J. Appl. Phys. **90**, 644 (2001).